Iraqi J. Laser, issue 2, vol., 20, pp. 18-23 (2021)

IRAQI JOURNAL OF LASER

The influence of no-core fibre length on the sensitivity Optical fibre Humidity sensor

Suroor L. khashin[1,*], Hanan J. Taher[1]

**Corresponding author:* Suroorlazem95@gmail.com

1. *Institute of Laser for Postgraduate Studies, University of Baghdad, Iraq, Baghdad, Iraq.*

(Received 14/10/2021; accepted 29/12/2021)

Abstract : Reflection optical fibre Humidity sensor is presented in this work, which is based on no core fibre prepared by splicing a segment of no core fibre (NCF) at different lengths 1-6 cm with fixed diameter 125 µm and a single mode fibre (SMF). The range of humidity inside the chamber is controlled from 30% to 90% RH at temperature ~ **30 °C**. The experimental result shows that the resonant wavelength dip shift decreases linearly with an increment of RH% and the sensitivity of the sensor increased linearly with an increasing in the length of NCF. However, a high sensitivity 716.07pm/RH% is obtained at length 5cm with good stability and reputability. Furthermore, the sensor is shifted towered a short wavelength (Blue shift).

Keywords: Optical Fibre sensor, RH sensor, No-core fibre, Circulator, Multimode Interference

1. Introduction

Relative humidity (RH) can be defined as the ratio of moisture content in the air to the total moisture (saturated) level that the air can carry at the same temperature [1]. Measuring RH is considered a significant importance parameter in a wide range of applications, such as bacterial growth, process control, product quality, food and beverage processing, automotive, and meteorological industries [2, 3]. Recently, optical fibre sensors have attracted extensive attentions in many fields of sensing, such as refractive index (RI) sensor [4], pH sensor [5], strain sensor [6], temperature sensor [7], curvature sensor [8], and humidity sensor [9]. Optical fibre humidity sensors have distinctive features such as being lightweight, small size, low cost, and having low attenuation and immunity to electromagnetic interference, making them an ideal sensing medium for several real-world applications [10, 11].

By measuring the changes in polarization, wavelength, phase and intensity of light passing through the sensing region, there are four types of optical fibre interferometer, namely Fabry-perot, Sagnac, Michelson, and Mach Zehnder interferometer. In 2016, Li-Peng Sun et. al. Proposed an optical fibre RH sensor based on a microfiber Sagnac loop interferometer, with a range of RH from 30%RH to 90%RH and sensitivity up to ~201.25 pm/%RH [12]. In 2021, CHENG ZHOU et. al., Proposed RH sensor that is based on sensitivity amplification and a reduction mechanism Internal–external Fabry–Perot cavity (IEFPC) and a range of humidity 40%–92% RH and sensitivity up to 715 pm/% RH [13]. In 2019, Piaopiao Wang et. al., Proposed a Methylcellulose (MC) film-coated RH sensor that is based on Michelson interferometer, with 30%-85% RH and sensitivity 133 pm/%RH [14]. In 2016, Suaad Sahib Hindal, Hanan J. Taher proposed an optical fibre RH sensor based on Photonic Crystal Fibre Interferometers (PCFIs) based on Mach Zehnder. The range of humidity in their proposal was 27% RH to 85% RH with a sensitivity of 5.86 pm / %RH [15]. In optical fibre humidity sensors (OFHS) based on MZI, the light is guided and modulated by a no core fibre and the surrounding medium, then is collected by a detector. As the RH is a function of the refractive index (RI), so any change in the RH effect on the transmitted or reflected light that passes through or interacts with the medium.

In this paper, a reflection optical fibre sensor is proposed and manufactured to be used to measure RH. The structure of the proposed sensor is easy, low cost and high sensitivity.

2. Experimental Work

2.1 Sensing Principle

Figure (1) shows the diagram of the proposed RH that is based on NCF (FG125LA from Thorlabs). It has a cladding with a diameter 125 µm, and SMF (corning SMF-28). The section of the NCF and SMF was spliced using a fusion splicer (Fujikura FSM-60S) [16]. The structure was made with a flat end of NCF using a cleaver. Different lengths of NCF were spliced with a single mode fiber. As shown in figure (1), the sensing beam is exposed to the surrounding medium while the reference beam is kept secluded. Any change in the surrounding medium will have an effect on the sensing beam, which induces phase difference. This phase shift generates a constructive or destructive interference pattern. As the light guided from SMF to the NCFs, the high order modes are excited and propagated within the NCF. These excited modes interfere with one another as they propagate along NCF length, giving rise to a multi-mode interference (MMI).

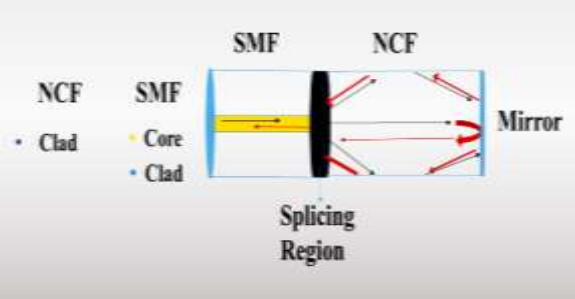

Figure (1): The structure of no core fiber (SNCF)

The reflected wavelength can calculate according to equation (1) [17]:

$$\lambda_{\circ} = p\left(\frac{nD^2}{2L}\right) \dots\dots\dots\dots\dots\dots\dots\dots\dots\dots\dots\dots\dots\dots (1)$$

where, $\lambda_{\circ}$ is the peak wavelength, n is the refractive index of the NCF, L is the length of the NCF, D is the diameter of the NCF, and p self-image, which is an integer number. When the light travel distance L over the NCF, a part of the light will escape as losses while a part of the light will collide at the end face of the fiber (mirror), then it reverses and travels a distance of 2L before coupling again at the SMF [18]. For different lengths, the self-image is formed when the modes travel along the NCFs, because of MMI effects. The initial mode is refocused at the length of the NCF.

2.2 Experimental set-up

Figure (2) shows the SNCF configuration. The system consists of a broadband source (BBS) with range 1450-1650nm (model: SLD1550S-A1 from Thorlabs) and circulator that contains three ports one of them is connected to BBS, and the second part is contacted to the optical spectrum analyzer OSA(YOKOKAWA, Ando AQ6370) with 0.02 nm resolution and the third port is connected to SNCF Humidity sensor.

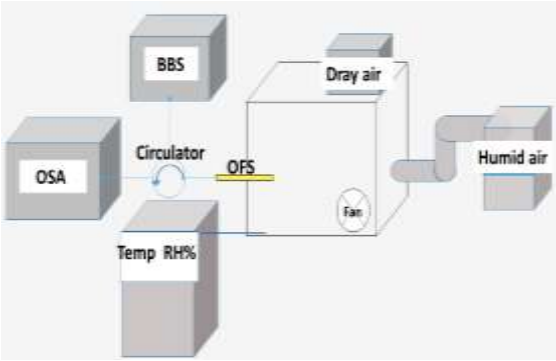

Figure (1): The experimental setup of the RH sensor.

SNCF is placed inside the chamber at different lengths of the NCF (1-6 cm). The chamber is placed in a plastic box that contains a small hole to allow the OFS entry inside the chamber. The chamber consists of three fans; one of these fans allows wet air to spread into the chamber while the other fans expel the air outside the chamber. An electronic RH meter is connected to the chamber to control the RH changes, in which the RH is slowly increased by 10% steps in the range 30 % - 90 % RH at approximately constant temperature of ~ 30 °C.

3. Results and discussion

In this work, OFHS has prepared by using different lengths of NCFs with diameter 125 μm. The structure is placed inside the chamber. At each RH, the reflection spectrum is measured after stabilizing for 10 seconds. It has been observed that the sensitivity is increased as the length of NCF is increased. Moreover, as the humidity increased the reflection spectrum shifted to a shorter wavelength (blue shift) where shown in figures (3-8).

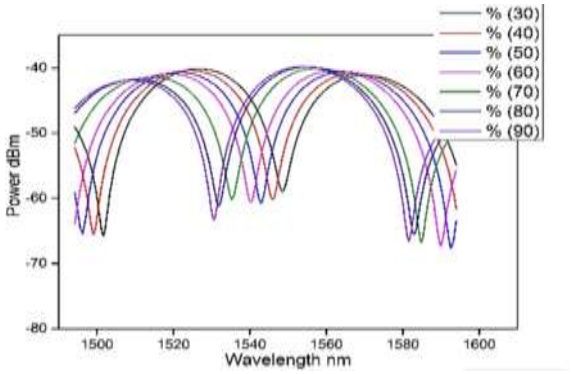

Figure (3): Reflection spectrum of NCFS for length 1 cm and diameter 125 μm.

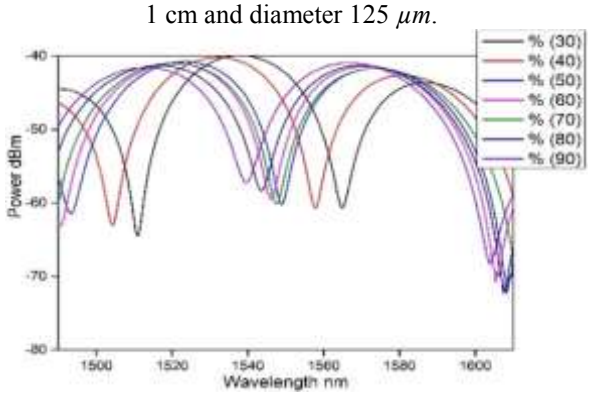

Figure (4): Reflection spectrum of NCFS for length 2 cm and diameter 125 μm.

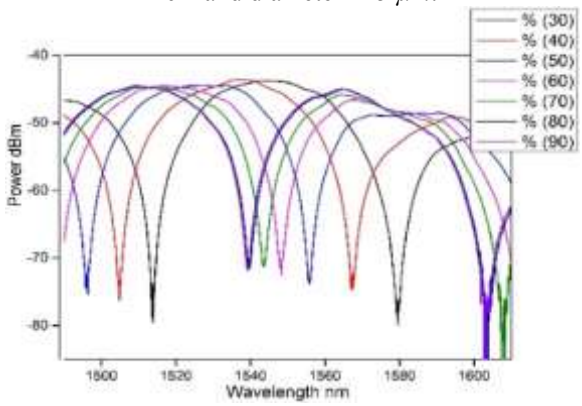

Figure (5): Reflection spectrum of NCFS for length 3 cm and diameter 125 μm.

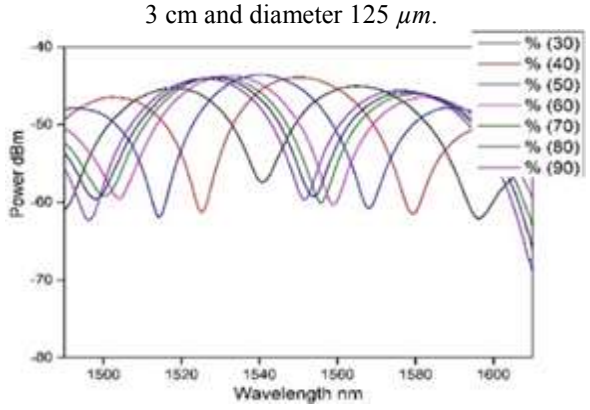

Figure (6): Reflection spectrum of NCFS for length 4 cm and diameter 125 μm.

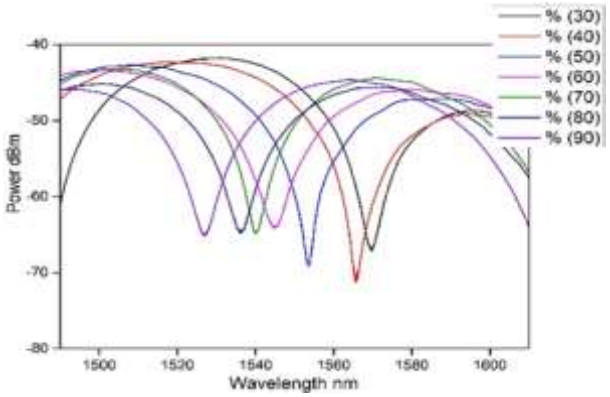

Figure (7): Reflection spectrum of NCFS for length 5 cm and diameter 125 μm.

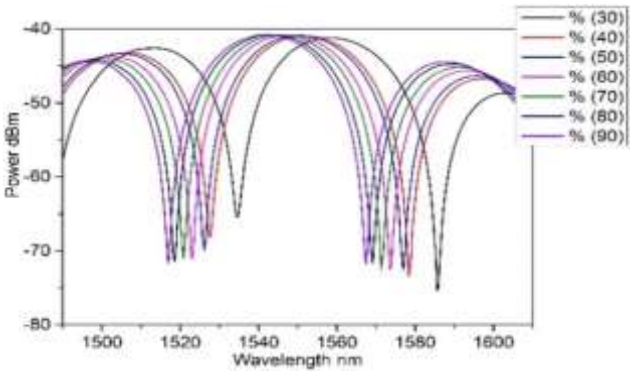

Figure (8): Reflection spectrum of NCFS for length 6 cm and diameter 125 μm.

Is shown in figures (9-14), the relation between linear fitting and RH% with rang 30%-90%. Any change in the length will have an effect on the sensitivity. When the length increases, an increase in the sensitivity is expected. For all lengths of NCFs, wavelength shift is approximately linear with an increase of relative humidity.

Table (1): lengths of NCFs with relative humidity

Length in cm	Sensitivity in pm/RH%
1	322.1
2	358.7
3	588.5
4	703.5
5	716.07
6	272.1

All lengths are shifted towered a short wavelength (blue shift). The highest sensitivity is reported as shown in figure (13), where the sensitivity was 716.07pm/RH% which was achieved at length 5 cm of NCF that reveals a

high wavelength shift causing a higher sensitivity for RH sensor. All lengths of NCFs were prepared without dip coats and they were uncoated.

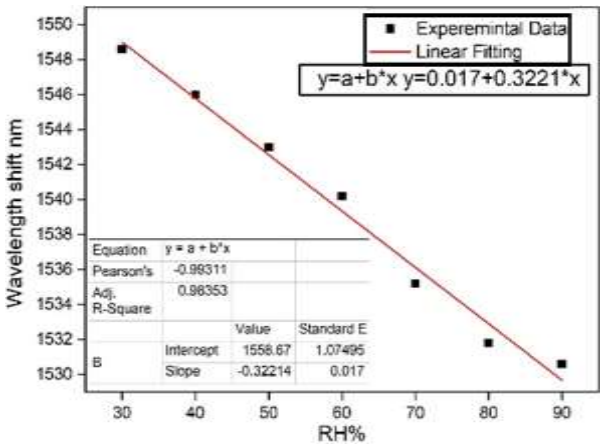

Figure (9): Linear fitting of NCFS for length 1 cm against RH% with sensitivity 322.1 pm/RH%.

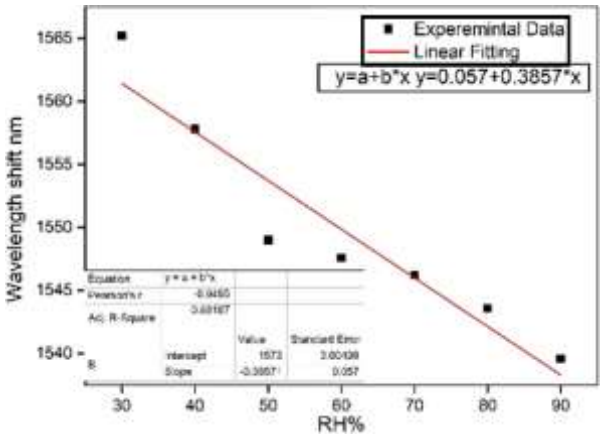

Figure (10): Linear fitting of NCFS for length 2 cm against RH% with sensitivity 385.7pm/RH%.

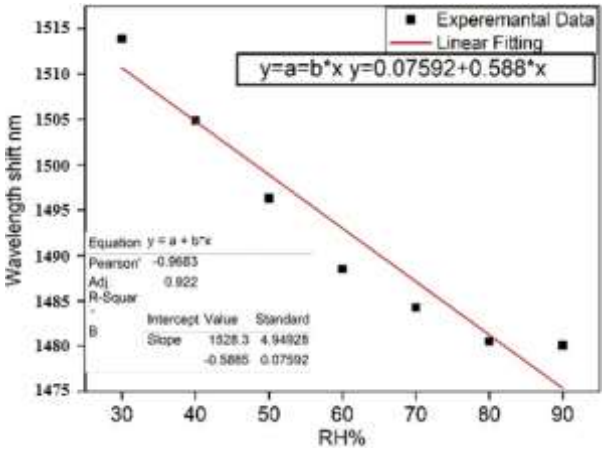

Figure (11): Linear fitting of NCFS for length 3 cm against RH% with sensitivity 588.5 pm/RH%.

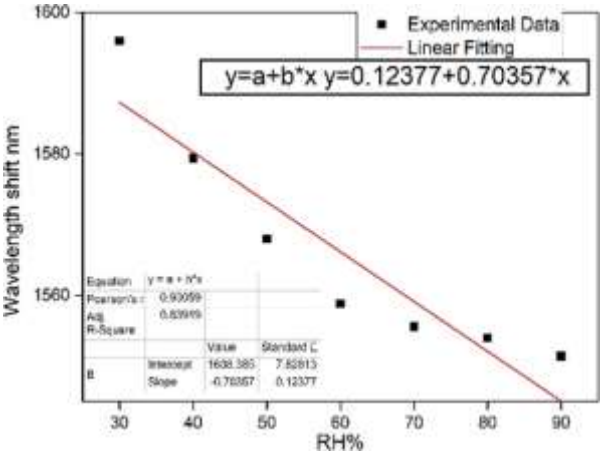

Figure (12): Linear fitting of NCFS for length 4 cm against RH% with sensitivity 703.5pm/RH%.

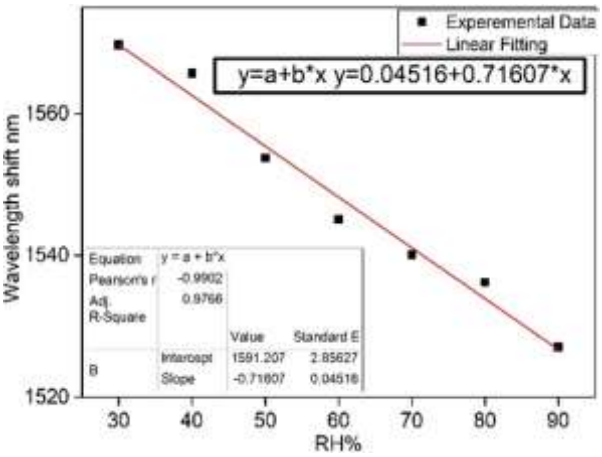

Figure (13): Linear fitting of NCFS for length 5cm against RH% with sensitivity 716.07 pm/RH%.

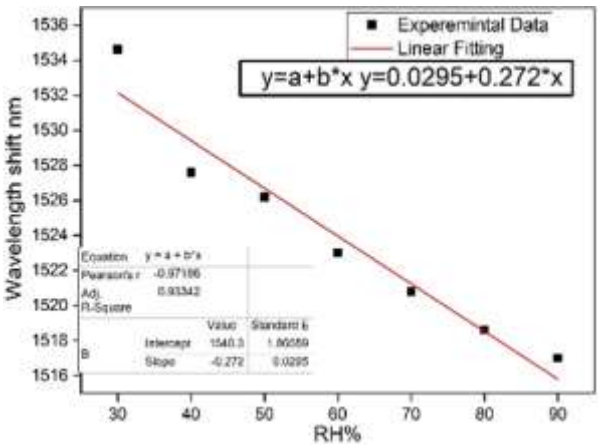

Figure (14): Linear fitting of NCFS for length 6 cm against RH% with sensitivity 272.1pm/RH%.

Figure (15), shows the relation between the sensitivity and the length of the NCF. As the length increases, the sensitivity is increased. The reason for this behavior can be interpreted as follows: when the effective area of the lengths

increases and the interaction between the water vapor and the cladding modes occurs that leads to getting a small phase shift between the interference modes. For a longer wavelength of 6 cm, the sensitivity will be decreased as at length 6 cm the interference will be diminution (distractive interference) which leads to an increase in the propagation losses of interference cladding modes. Additionally, in a length of 6 cm, the spacing of the fringe will be narrow, which causes a limited measurement range.

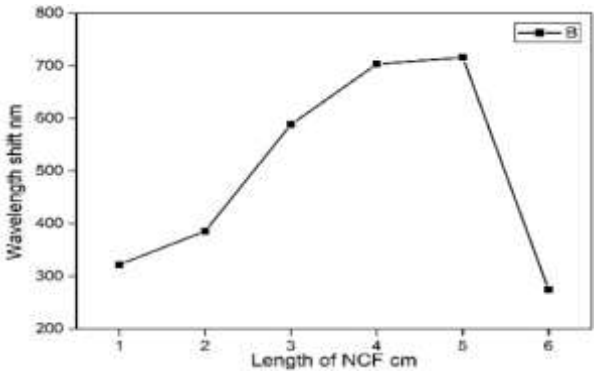

Figure (15): Relation between sensitivity in Pm/RH and the change in length of the NCF in cm.

Stability and reputability are another important conditions in the operation system of any sensor. The results of the spectrum shift as a function of RH were recorded in two different ways with increasing and decreasing RH that are shown in figure (16). The difference between the measurements was one day and the sensor still works normally with good stability and repeatability.

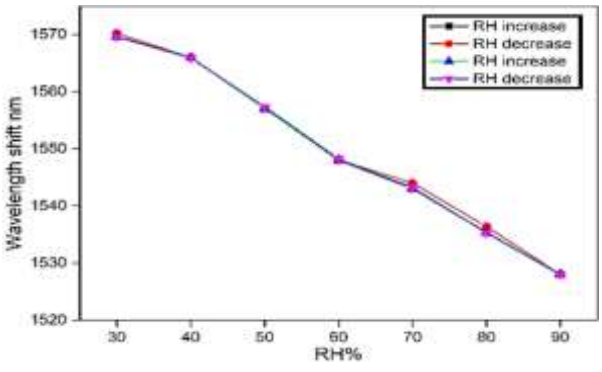

Figure (16): Humidity stability and Reputability.

4. Conclusion

In summary, a simple reflective optical fibre humidity sensor based on no core fibre (NCF) prepared. The structure has been fabricated by using different lengths of NCF with diameter 125μ where splicing to SMF. The end of NCF has cleaved to get a flat (mirror) end. Humidity (RH) ranged 30%-90% at temperature ~ 30 °C.

As the humidity increases, the reflection spectrum of the sensor moved toward the short wave direction (blue shift). The sensitivity increase as the length increases from the length 1 cm to length 5 cm. The sensitivity was increased 322.1 pm/RH%, 385 pm/RH%. 7,588.5 pm/RH%, 703.5 pm/RH%, 716.07 pm/RH%, and 272.1 pm/RH% at a length of 6cm. It can be concluded the highest sensitivity is achieved 716.07 pm/RH% at the length of 5 cm, and at length 6 cm the sensitivity will be decreased to 272.1 pm/RH%. This is because at a length 6 cm, the propagation losses of interference cladding modes are increased. Furthermore, the spacing of the fringe will be narrow, which causes limited measurement, and hence the sensitivity is decreased. The proposed humidity sensor shows good repeatability and stability with high sensitivity.

5. Reference

[1] Hamid Farahani , Rahman Wagiran and Mohd Nizar Hamidon "Humidity Sensors Principle, Mechanism, and Fabrication Technologies: A Comprehensive Review". Sensors. 14, 7881-7939, 2014.

[2] Zhang, Z.F.; Zhang, Y. "Humidity sensor based on optical fiber attached with hydrogel spheres". Opt. Laser Technol. 74, 16–19, 2015.

[3] Torres, D.L.; Elousa, C.; Villatoro, J.; Zubiac, J.; Rothhardt, M.; Schuster, K.; Arregui, F.J. "Enhancing sensitivity of photonic crystal fiber interferometric humidity sensor by the thickness of SnO2 thin films". Sens. Actuators B Chem. 251, 1059–1067,2017.

[4] Y. Zhao, X.G. Li, L. Cai, et al., "Measurement of RI and temperature using composite interferometer with hollow-core Fiber and photonic crystal fiber", IEEE Trans. Instrum. Meas. 65 (11), 2631–2636,2016,

[5] Y. Zheng, L.H. Chen, X. Dong, et al., Miniature pH optical Fiber sensor based on Fabry–Perot interferometer, IEEE J. Sel. Top. Quantum Electron. 22(2), 1–5, 2016.

[6] Y. Sun, D. Liu, P. Lu, et al., "High sensitivity optical fiber strain sensor using

twisted multimode fiber based on SMS structure", Opt. Commun. 405, 416–420 2017.
[7] S. Wu, G. Yan, Z. Lian, et al., "An open-cavity Fabry–Perot interferometer with PVA coating for simultaneous measurement of relative humidity and temperature", Sensors Actuators B 225, 50–56,2016.
[8] Z. Shao, X. Qiao, W. Bao, et al., "Temperature-independent gas refractometer based on an S-taper fiber tailored fiber Bragg grating", Opt. Commun. 374, 34–38 2016.
[9] Q. Hu, S. Zhang, W. Yang, et al., "Highly sensitive curvature sensor based on long period fiber grating with alternately splicing multiple single/multimode structure", Opt. Fiber Technol., Mater. Devices Syst. 37, 69–73 2017.
[10] Rajan,G. "Advanced Techniques and Applications", Optical Fiber Sensors 1st ed.; CRC Press: Boca Raton, FL, USA, 2015.
[11] Hartog, A. "An Introduction to Distributed Optical Fibre Sensors", 1st ed.; CRC Press: Boca Raton, FL, USA, 2017.
[12] Li-Peng Sun, Jie Li, Long Jin, Yang Ran, Bai-Ou Guan. "High-birefringence microfiber Sagnac interferometer based humidity sensor", Sensors and Actuators B231, 696-700, 2016.
[13] Cheng Zhou, Qian Zhou, Bo Wang, Jiajun Tian, and Yong Yao. "High-sensitivity relative humidity fiber-optic sensor based on an internal–external Fabry–Perot cavity Vernier effect". Optics Express, Vol. 29, No. 8, 11854, 2021.
[14] Piaopiao Wanga, Kai Ni, Bowen Wanga, Qifei Maa, Weijian Tian. "Methylcellulose coated humidity sensor based on Michelson interferometer with thin-core fiber". Sensors and Actuators, A288, 75-78, 2019.
[15] Suaad Sahib Hindal, Hanan J. Taher. "Performance of humidity sensor based on photonic crystal fiber interferometer". Iraqi Journal of Physics,Vol.14, No.30, PP. 83-89, 2016.
[16] Huda T. Al-Swefee, Sarah K. Al-Hayali and Abdulhadi A. Al-Janabi."Enhanced Relative Humidity Sensor via Diameter of No-Core Fiber Structure". Iraqi J. Laser, No.1, Vol.18, pp.19-23, 2019.
[17] Socorro, A.B.; Del Villar, I.; Corres, J.M.; Arregui, F.J.; Matias, "I.R. Mode transition in complex refractive index coated single-mode–multimode–single-mode structure". Opt. Express, 21, 12668–12682, 2013.
[18] Wang, Q.; Farrell, G. "All-fiber multimode-interference- base refractometer sensor: Proposal and design". Opt. Lett. 31, 317–319, 2006.

تأثير التغيير في الطول للالياف المنزوعة اللب لقياس التحسس للرطوبة النسبية

سرور لازم ,حنان جعفر.

معهد الليزر للدراسات العليا، جامعة بغداد، بغداد، العراق

الخلاصة: تم بناء متحسس للرطوبة النسبية الذي يعمل في نمط الانعكاس، حيث تم تصنيع المتحسس باستخدام أطوال مختلفة من الألياف منزوعة القلب ذات أطوال مختلفة (1-6) سم وقطر ثابت 125مايكروميتر ذو نهايات مسطحة ولحامها مع ليف بصري أحادي. تم ضبط الرطوبة داخل الجهاز لقياس الرطوبة (30%-90%) بدرجة حرارة مقاربة 30سيلزي.أضهرت النتائج المختبرية أن قمم التداخل تقل تدريجيا مع زيادة نسبة الرطوبة والتحسس يزداد بزيادة الطول للألياف منزوعة القلب. حيث إن قمم التداخل تزحزحت نحو الأطوال الموجية القصيرة مع زيادة مقدار الرطوبة. تزداد التحسس عند زيادة الطول للألياف منزوعة القلب حيث كانت اعلى قيمة للتحسس (716.07بيكومتر/النسبة المئوية للرطوبة النسية) للطول 5 سم. اظهر المتحسس استقراريه عالية. يمتاز متحسس الرطوبة المصمم بأنه ذو حجم صغير، سهولة تصنيع وحساسية عالية.